Title

Proteomic profiling of Pachyonychia congenita plantar callus

Authors

Rice, Robert H

Durbin-Johnson, Blythe P

Salemi, Michelle

et al.

Publication Date

2017-08-01

DOI

10.1016/j.jprot.2017.06.017

Peer reviewed

HHS Public Access

Author manuscript

J Proteomics. Author manuscript; available in PMC 2018 August 08.

Published in final edited form as:

J Proteomics. 2017 August 08; 165: 132–137. doi:10.1016/j.jprot.2017.06.017.

Proteomic profiling of Pachyonychia congenita plantar callus

Robert H. Rice[a,*], **Blythe P. Durbin-Johnson**[b], **Michelle Salemi**[c], **Mary E. Schwartz**[d], **David M. Rocke**[b], and **Brett S. Phinney**[c]

[a]Department of Environmental Toxicology, University of California, Davis, CA

[b]Division of Biostatistics, Department of Public Health Sciences, Clinical and Translational Science Center Biostatistics Core, University of California, Davis, CA

[c]Proteomics Core Facility, University of California, Davis, CA

[d]PC Project, Salt Lake City, UT

Abstract

Callus samples from the ball and the arch of the foot, collected on tape circles, were compared by shotgun proteomic profiling. Pachyonychia congenita subjects were sampled who exhibited a mutation in *KRT6A, KRT6B, KRT6C, KRT16* or *KRT17*, and the proteins were digested and analyzed by tandem mass spectrometry. In comparison with samples from unaffected control subjects, those from subjects with *KRT6A* or *KRT16* mutations displayed the most differences in profile from normal, while those from subjects with *KRT6C* or *KRT17* mutations showed few differences from normal. The profiles from subjects with *KRT6B* mutations were intermediate in protein profile differences. Degree of departure from the normal profile could be estimated by expression of numerous proteins in callus from the ball of the foot that were consistently different. By contrast, the protein profile from the arch of the foot was hardly affected. The results provide a foundation for noninvasive monitoring of the efficacy of treatments with quantitative assessment of departure from the normal phenotype.

Graphical abstract

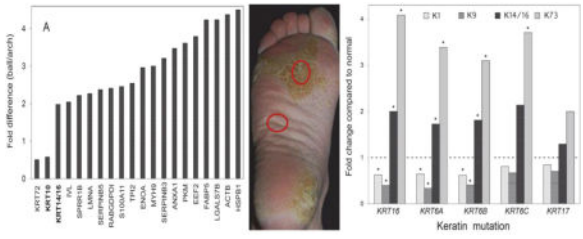

*Corresponding author: Department of Environmental Toxicology, University of California, Davis, CA 95616-8588; Tel 530-752-5176; Fax 530-752-3394; rhrice@ucdavis.edu.

Conflict of Interest

All authors declare they have no conflict of interest.

Keywords

Human plantar callus; Keratin mutations; Pachyonychia congenita

1. Introduction

Pachyonychia congenita (PC) is characterized by palmoplantar keratoderma and abnormalities of the nail unit, generally appearing within the first decade of life [1]. Other symptoms can include mucosal leukokeratosis, follicular hyperkeratosis, cysts, hoarseness, hyperhidrosis and natal teeth [2]. The most important feature affecting the quality of life is the pain associated with plantar hyperkeratosis, which can severely restrict mobility, and the abnormal appearance of the nail unit has a negative impact, particularly in adolescence [3]. Genetic testing has led to recognition that the syndrome results from a mutation in *KRT6A, KRT6B, KRT6C, KRT16* or *KRT17* [4]. The mutation is transmitted in an autosomal dominant fashion, representing a gain of function, such as interfering with keratin filament formation, demonstrated for a mutation in *KRT6C* [5], and loss of barrier integrity. However, the observation that *Krt16* null mice exhibit palmoplantar keratoderma point to a possible additional, recessive origin for this syndrome [6] not yet obvious in humans.

Protein profiling is now capable of demonstrating major perturbations in epidermis and corneocytes from mouse models of genetic defects [7–9]. Such analysis has shown that the profile of human lamellar ichthyosis epidermis with defective TGM1 is distinct from normal and preserved upon grafting to the mouse [10]. They also permit distinguishing the profiles of lamellar ichthyosis from ichthyosis vulgaris and normal epidermis [11]. Initial application to PC, generally supporting findings obtained by DNA microarray, indicate that mutation of *KRT6A* leads to readily detectable perturbations in levels of several keratins and other proteins [12]. Present work explores the perturbations more generally in plantar epidermis among PC subjects for possible applications to understanding the disease pathogenesis and to assessment of treatment.

2. Materials and methods

2.1 Sampling

Subjects (6 normal controls, 9 with *KRT6A* mutations, 5 with *KRT6B* mutations, 3 with *KRT6C* mutations, 10 with *KRT16* mutations, 5 with *KRT17* mutations; see supplementary Table S1) were recruited with informed consent by the Pachyonychia Congenita Project (http://pachyonychia.org). In their own homes, subjects wiped with alcohol the areas of the foot sole to be sampled. After air drying, each site was sampled (applied using tweezers and pressed against the skin with circular motion using a gloved finger) with three 22 mm diameter D-Squame Pro tape circles (CuDerm Corp, Dallas, TX). The most superficial layer of corneocytes adheres to the adhesive on the bottom of each tape circle. Unaffected areas (no blisters/calluses) in the arch region and affected areas (with blisters/calluses) from the ball of the foot were sampled from the same subjects. Normal subjects sampled the same regions. The three circles for each site were placed in a new 15 ml plastic sterile cell culture centrifuge tube (two tubes per subject) and the cap was tightly affixed. The samples were

collected from subjects by the Pachyonychia Congenita Project and mailed together to the University of California Davis for processing and analysis.

2.2 Sample processing

After the tape circles (three per site) were immersed in 2% SDS – 0.1 M sodium phosphate (pH 7.8) for a day, the eluted corneocytes were collected by centrifugation and rinsed twice with water. The pellets were rinsed with 2% sodium dodecanoate – 50 mM ammonium bicarbonate, resuspended in 0.5 ml of this buffer adjusted to 25 mM dithioerythritol, heated 10 min in a 95°C water bath and incubated at room temperature with stirring for 45 min. Samples were then stirred at room temperature for 45 min in the dark after addition of iodoacetamide to 50 mM. The pH was adjusted to 3 with 8 μl of trifluoroacetic acid, and the samples were extracted three times with ethyl acetate. The pH was then adjusted to 8 with 2.5 μl of ammonia and 25 μl of 1 M ammonium bicarbonate, after which were added 20 μg of reductively methylated bovine trypsin daily, and the digest was gently stirred magnetically for a total of three days. The digests were then clarified by centrifugation and submitted for mass spectrometric analysis.

2.3 Mass spectrometry

Digested protein samples were block randomized into 10 blocks, and the digested peptides were analyzed by LC-MS/MS on a Thermo Scientific Q Exactive+ Orbitrap Mass spectrometer in conjunction with a Proxeon Easy-nLC II HPLC (Thermo Scientific) and Proxeon nanospray source. Peptides were loaded on a 100 micron × 25 mm Magic C18 100Å 5U reverse phase trap where they were desalted online before being separated using a 75 micron × 150 mm Magic C18 200Å 3U reverse phase column. Peptides were eluted using a 120 minute gradient with a flow rate of 300 nl/min. An MS survey scan was obtained for the m/z range 350–1600, MS/MS spectra were acquired using a top 15 method, where the top 15 ions in the MS spectra were subjected to HCD (High Energy Collisional Dissociation). An isolation mass window of 2.0 m/z was employed for precursor ion selection, and normalized collision energy of 27% was used for fragmentation. A five second duration was used for dynamic exclusion.

2.4 Database searching

Tandem mass spectra were extracted by Proteome Discoverer version 1.2. Charge state deconvolution and deisotoping were not performed. All MS/MS samples were analyzed using X! Tandem (The GPM, thegpm.org; version X! Tandem Sledgehammer, 2013.09.01.2). X! Tandem was set up to search the NCBI human refseq database (Feb 2015) and all non-human common laboratory contaminants (http://www.thegpm.org/crap/) and an equal number of reverse sequences (144593 entries total) assuming the digestion enzyme trypsin. X! Tandem was searched with a fragment ion mass tolerance of 20 PPM and a parent ion tolerance of 10.0 PPM. 57.021464@U of selenocysteine and carbamidomethyl of cysteine were specified in X! Tandem as fixed modifications. Glu->pyro-Glu of the N-terminus, ammonia-loss of the N-terminus, Gln->pyro-Glu of the N-terminus, deamidation of asparagine and glutamine, oxidation of methionine and tryptophan and dioxidation of methionine and tryptophan were specified in X! Tandem as variable modifications.

2.5 Criteria for protein identification

Scaffold (version Scaffold_4.7.5, Proteome Software Inc., Portland, OR) was used to validate MS/MS based peptide and protein identifications. Peptide identifications were accepted if they could achieve a peptide threshold of 97% using Scaffold's LFDR algorithm and protein identifications were accepted if they contained at least two peptides at this threshold. This resulted in an overall peptide decoy FDR of 0.0% and a protein decoy FDR of 0.7%. Proteins that contained similar peptides and could not be differentiated based on MS/MS analysis alone were grouped to satisfy principles of parsimony. Proteins sharing significant peptide evidence were grouped into clusters, where spectral counts were adjusted for shared peptides. Spectral counts of exclusive peptides (present in only one protein) were compiled and compared to the weighted counts (adjusted according to the number of other proteins sharing the same peptide sequence) to permit removal of a small fraction of the proteins with many more weighted than exclusive counts and thus not certain to be present. The Scaffold file containing all the peptide data used in the analysis is available on the MassIVE repository (http://massive.ucsd.edu) MassIVE ID = MSV000080891.

2.6 Statistical analysis

Proteins or clusters with an average count less than 1 across samples were filtered prior to analysis. Count data were transformed using a variance stabilizing transformation for negative binomial data, which takes the form $f_\theta(x) = \ln [x + (x^2 + x/\theta)^{0.5} + 1/2\theta]$. This transformation, when θ is selected to minimize the correlation between the variance and standard deviation of the transformed data, removes mean-variance dependency from the data so that they may be analyzed assuming constant variance across the range of the data. Data were then analyzed using the Bioconductor package for gene expression analysis limma [13], which fits linear models to each protein separately then applies empirical Bayes shrinkage to the estimated variances in order to increase power. The linear model used included effects for location, genotype, and their interaction, and a random effect for subject in order to address sample pairing. Tests for differences between genotypes in arch samples, in ball samples, and in general were conducted as contrasts of this model. The application of the above transformation to RNA-Seq data is discussed in Rocke et al. (http://biorxiv.org/content/biorxiv/early/2015/06/11/020784.full.pdf). The overall analysis approach is similar to that called "limma-trans" in [14], which employs the variance stabilizing transformation from the DESeq RNA-Seq analysis package [15]. Analyses were conducted using R, version 3.1.3 [16].

3. Results

To provide a baseline for comparisons among samples, since epidermal profiles differ at anatomic sites [11], the profiles of the ball and arch of the foot were compared among normal control subjects. Of the 173 proteins subjected to statistical analysis, 20 were seen to be significantly different in pairwise comparisons (Figure 1A). Of these, K10 and K14/16 were highly prevalent, with spectral counts an order of magnitude greater than the rest. The weighted spectral counts for K10 were only half as high in samples from the ball of the foot as in samples from the arch, whereas the counts of K14/16 were twice as high in the ball as in the arch samples. The high variance among the samples analyzed, as seen in Figure 1B,

reflects the considerable variability in profile among individuals, as noted previously [11]. While K14 and K16 were analyzed as a cluster due to their shared peptides, they exhibited parallel differences between arch and ball of the foot as seen by analysis of their exclusive peptides (Figure 1C). These results, consistent with our previous study of different epidermal sites, indicate that comparison of the normal and PC samples are best conducted comparing the same anatomic site.

To detect differences from normal and among the various mutation categories, protein profiles for the ball of the foot from control and PC patients, aggregated by keratin mutation, were subjected to two way comparisons. As shown in Table 1A, samples from subjects with *KRT6A* or *KRT16* mutations showed wide divergence in protein profile from samples provided by normal controls subjects. While ≈100 of the 173 proteins analyzed differed significantly in spectral counts in two way comparisons with normal, samples from subjects with the *KRT6A* or *KRT16* mutations differed little from each other. By contrast, samples from subjects with mutations in *KRT6C* or *KRT17* exhibited few differences in two way comparisons with normal (2 or 4, respectively), and also did not show differences from each other. Samples from subjects with *KRT6B* mutations displayed an intermediate number of differences in two way comparisons with normal (36), a small number of differences from samples with *KRT6A* and *KRT16* mutations (7 or 6, respectively) and none from samples provided by individuals with *KRT6C* and *KRT17* mutations. By contrast, as shown in Table 1B, few proteins differed in the two way comparisons of arch samples from control and PC subjects.

As suggested by the results above, samples from subjects with different keratin mutations showed considerable overlap in proteins by which they differed from normal controls. To find the degree to which this was the case, the proteins that differed were compared. As shown in Table 2, comparison of the profiles showed that most of the proteins differing from normal in samples from subjects with mutant *KRT6A* and *KRT16* were the same (90). Similarly, virtually all of the proteins differing from normal from subjects with *KRT6B* and *KRT6C* mutations were also different in those from samples with *KRT6A* and *KTR16* mutations. The few differences from normal observed in samples with *KRT17* mutations (4) were seen to varying extents in the other samples (0–4).

Among the proteins with the largest absolute differences in expression level between normal and diseased were certain keratins that were expressed at high levels. In samples mutated in *KRT6A*, *KRT6B* and *KTR16*, as shown in Figure 2, K1 and K9 levels were suppressed approximately by half, while K14/16 levels were stimulated two fold and K73 (though much lower in spectral counts) was stimulated 3–4 fold. (The differences in relative number of spectral counts are shown in Figure S1.) Although not statistically significant in most cases, differences in expression level in the same direction were noted for samples with mutant *KRT6C* and *KRT17*. In all cases, as judged by exclusive spectral counts, differences seen in expression levels of K14 and K16 were parallel to the value for the cluster. However, the degrees of difference from normal in K16 in each case were nearly double those seen in K14.

Of the proteins judged significantly altered in samples from subjects with *KRT6A* and *KRT16* mutations, 8 were judged to be lower in expression level than normal. In addition to K1 and K9 illustrated in Figure 2, the other 6 (CDSN, DSC1, CAT, ECM1, DCD2, DSG1) are illustrated in Figure 3A. Although not significantly altered in samples with *KRT6B*, *KRT6C* and *KRT17* mutations, a trend was evident where the values were noticeably lower than in control samples. To examine whether a corresponding trend was evident in proteins with higher expression levels in PC samples, 15 of the proteins with the highest deviations from normal were examined. As shown in Figure 3B–3D, a gradient was apparent where the degree of deviation was lower in the direction of *KRT16*, *KRT6A*, *KRT6B*, *KRT6C* and *KRT17*. The differences are illustrated as fold change from control in Figure 3 and in relative numbers of spectral counts in Figure S2.

4. Discussion

Understanding the molecular basis of the keratinopathies was greatly facilitated by findings that mutant keratins can disrupt the cytoskeletal network in cell culture [17] and in transgenic mice [18]. From such observations in many laboratories [19], the keratin cytoskeleton is demonstrably critical for structural stability within keratinocytes. Through interactions with desmosomes, keratins are important for proper intercellular adhesion, and they are major participants in cross-linked envelope formation [8, 9]. Such work helps understand how impairment of the barrier function could rationalize development of the observed keratoderma in PC [20].

A simple hypothesis to rationalize the sites that are most affected by PC mutations is that the affected keratins are most highly expressed at those sites [4]. Relative levels of different proteins are not easily judged from spectral counts, especially in view of substantial peptide sharing in K6A, K6B and K6C. Estimates using iBAQ values from Maxquant intensity data indicate that K9 and K1 together account for over half the total protein in callus from the ball of the foot (Table S2), while K6a, K6b, K6c, K16 and K17 each account for an order of magnitude less protein. However, levels in the basal and spinous layers may differ considerably from those observed in the superficial callus. Consistent with PC symptoms commonly showing effects on nail plate, proteomic profiling of the latter from human finger reveals similar or slightly higher levels of K17 compared to K6 and K16 [21]. In any case, that mutations in *KRT6C* and *KRT17* produce few alterations in protein level in the ball of the foot in this study is consistent with observations that these mutations often have milder clinical effects.

The significance of the present proteomic profiling results is unclear for understanding the generation of severe plantar pain in PC, which may be as important for mutations in *KRT17* as in *KRT6A* [22]. This difficulty may reflect the participation by keratins in various signaling pathways and in cell migration [23] or keratin-specific feedback mechanisms. Deletion of some keratins can lead to oxidative stress, to which perturbation of certain signaling pathways [24] and alteration of mitochondrial lipids and protein may contribute [8]. Whether such perturbation leads to pain sensitization in the epidermis and, if so, how (e.g., secretion of neurotrophic factors), or whether an effect on the skin architecture is involved, is unknown [25].

5. Conclusion

Despite a lack of direct relevance to pain generation, proteomic profiling could provide a quantitative foundation for judging effectiveness of treatment regimens [12]. As observed in other proteomic studies of epidermis [9] and hair [26], changes in a single gene can profoundly alter the protein profile. Indeed, alterations in the profiles are distributed among many protein functional categories in the cell. For the present purpose, observed perturbations of many proteins, including K1, K9, K16 and K73 are available for noninvasive monitoring using tape circles as demonstrated here. Moreover, since inter-individual differences can be quite large in population studies such as this one, sampling of single individuals for this purpose could provide more dramatic shifts as the treated epidermis approaches a normal phenotype than the averages reported here.

Supplementary Material

Refer to Web version on PubMed Central for supplementary material.

Acknowledgments

We thank Dr. Leonard M. Milstone for encouraging this study, Ms. Holly Evans for help with data preparation and the subjects for their cooperation. The funding sources had no role in data analysis and interpretation, writing this report or its submission for publication.

Funding

The Pachyonychia Congenita Project and the National Center for Advancing Translational Sciences (NIH grant UL1 TR001860) provided financial support.

References

1. Eliason MJ, Leachman SA, Feng BJ, Schwartz ME, Hansen CD. A review of the clinical phenotype of 254 patients with genetically confirmed pachyonychia congenita. J Am Acad Dermatol. 2012; 67:680–6. [PubMed: 22264670]
2. Leachman SA, Kaspar RL, Fleckman P, Florell SR, Smith FJ, McLean WH, et al. Clinical and pathological features of pachyonychia congenita. J Invest Dermatol Symp Proc. 2005; 10:3–17.
3. Shah S, Boen M, Kenner-Bell B, Schwartz M, Rademaker A, Paller AS. Pachyonychia congenita in pediatric patients. Natural history, features, and impact. JAMA Dermatol. 2014; 150:146–53. [PubMed: 24132595]
4. Wilson NJ, O'Toole EA, Milstone LM, Hansen CD, Shepherd AA, Al-Asadi E, et al. The molecular genetic analysis of the expanding pachyonychia congenita case collection. Br J Dermatol. 2014; 171:343–55. [PubMed: 24611874]
5. Kubo A, Oura Y, Hirano T, Aoyama Y, Sato S, Nakamura K, et al. Collapse of the keratin filament network through the expression of mutant keratin 6c observed in a case of focal plantar keratoderma. J Dermatol. 2013; 40:553–7. [PubMed: 23662636]
6. Lessard JC, Coulombe PA. Keratin 16–null mice develop palmoplantar keratoderma, a hallmark feature of pachyonychia congenita and related disorders. J Invest Dermatol. 2012; 132:1384–91. [PubMed: 22336941]
7. Rorke E, Gautam A, Young C, Rice R, Elias P, Crumrine D, et al. Structural and biochemical changes underlying a keratoderma-like phenotype in mice lacking suprabasal AP1 transcription factor function. Cell Death Dis. 2015; 6:e1647. [PubMed: 25695600]
8. Kumar V, Bouameur J-E, Bär J, Rice RH, Hornig-Do H-T, Roop DR, et al. A keratin scaffold regulates epidermal barrier formation, mitochondrial lipid composition and activity. J Cell Biol. 2015; 211:1057–75. [PubMed: 26644517]

9. Rice RH, Durbin-Johnson BP, Ishitsuka YI, Salemi M, Phinney BS, Rocke DM, et al. Proteomic analysis of loricrin knockout mouse epidermis. J Proteome Res. 2016; 15:2560–6. [PubMed: 27418529]
10. Aufenvenne K, Rice RH, Hausser I, Oji V, Hennies HC, Rio MD, et al. Long-term faithful recapitulation of transglutaminase 1-deficient lamellar ichthyosis in a skin-humanized mouse model, and insights from proteomic studies. J Invest Dermatol. 2012; 132:1918–21. [PubMed: 22437313]
11. Rice RH, Bradshaw KM, Durbin-Johnson BP, Rocke DM, Eigenheer RA, Phinney BS, et al. Distinguishing ichthyoses by protein profiling. PLoS One. 2013; 8(10):e75355. [PubMed: 24130705]
12. Cao Y-A, Hickerson RP, Seegmiller BL, Grapov D, Gross MM, Bessette MR, et al. Gene expression profiling in pachyonychia congenita skin. J Dermatol Sci. 2015; 77:156–65. [PubMed: 25656049]
13. Ritchie ME, Phipson B, Wu D, Hu Y, Law CW, Shi W, et al. limma powers differential expression analyses for RNA-sequencing and microarray studies. Nucl Acids Res. 2015; 43doi: 10.1093/nar/gkv007
14. Soneson C, Delorenzi M. A comparison of methods for differential expression analysis of RNA-seq data. BMC bioinformatics. 2013; 14(1):91. [PubMed: 23497356]
15. Anders S, Huber W. Differential expression analysis for sequence count data. Genome Biol. 2010; 11:R106. [PubMed: 20979621]
16. R Core Team. R: A language and environment for statistical computing. Vienna, Austria: R Foundation for Statistical Computing; 2015.
17. Albers K, Fuchs E. The expression of mutant epidermal keratin cDNAs transfected in simple epithelial and squamous cell carcinoma lines. J Cell Biol. 1987; 105:791–806. [PubMed: 2442174]
18. Vassar R, Coulombe PA, Degenstein L, Albers K, Fuchs E. Mutant keratin expression in transgenic mice causes marked abnormalities resembling a human genetic skin disease. Cell. 1991; 64:365–80. [PubMed: 1703046]
19. Tan TS, Ng YZ, Badowski C, Dang T, Common JE, Lacina L, et al. Assays to study consequences of cytoplasmic intermediate filament mutations: the case of epidermal keratins. Meth Enzymol. 2016; 568:219–53. [PubMed: 26795473]
20. Schmuth M, Gruber R, Elias PM, Williams ML. Ichthyosis update: towards a function-driven model of pathogenesis of the disorders of cornification and the role of corneocyte proteins in these disorders. Adv Dermatol. 2007; 23:231–56. [PubMed: 18159904]
21. Rice RH, Xia Y, Alvarado RJ, Phinney BS. Proteomic analysis of human nail plate. J Proteome Res. 2010; 9:6752–8. [PubMed: 20939611]
22. Wallis T, Poole CD, Hoggart B. Can skin disease cause neuropathic pain? A study in pachyonychia congenita. Clin Exp Dermatol. 2016; 41:26–33. [PubMed: 26358843]
23. Toivola DM, Boor P, Alam C, Strnad P. Keratins in health and disease. Curr Opin Cell Biol. 2015; 32:73–81. [PubMed: 25599598]
24. Kerns ML, Hakim JMC, Lu RG, Berroth A, Kaspar RL, Coulombe PA. Oxidative stress and dysfunctional NRF2 underlie pachyonychia congenita phenotypes. J Clin Invest. 2016; 126:2356–66. [PubMed: 27183391]
25. Pan B, Byrnes K, Schwartz M, Hansen CD, Campbell CM, Krupiczojc M, et al. Peripheral neuropathic changes in pachyonychia congenita. Pain. 2016; 157:2843–53. [PubMed: 27776012]
26. Rice RH, Bradshaw KM, Durbin-Johnson BP, Rocke DM, Eigenheer RA, Phinney BS, et al. Differentiating inbred mouse strains from each other and those with single gene mutations using hair proteomics. PLoS One. 2012; 7:e51956. [PubMed: 23251662]

Significance

Pachyonychia congenita is an orphan disease in which the connection between the basic defect (keratin mutation) and debilitating symptoms (severe plantar pain) is poorly understood. Present work addresses the degree to which the protein profile is altered in the epidermis where the severe pain originates. The results indicate that the mutated keratins differ greatly in the degree to which they elicit perturbations in protein profile. In those cases with markedly altered protein levels, monitoring the callus profile may provide an objective measure of treatment efficacy.

Highlights

- Protein profiles of the arch and ball of the foot were distinguishable.
- The KRT mutations had little effect on protein profile of the arch.
- Samples of ball of the foot with mutated *KRT6A* or *KRT16* had many protein alterations.
- Samples with mutated *KRT6A* or *KRT16* exhibited many perturbations in common.
- Samples with *KRT6C* or *KRT17* had few protein alterations.

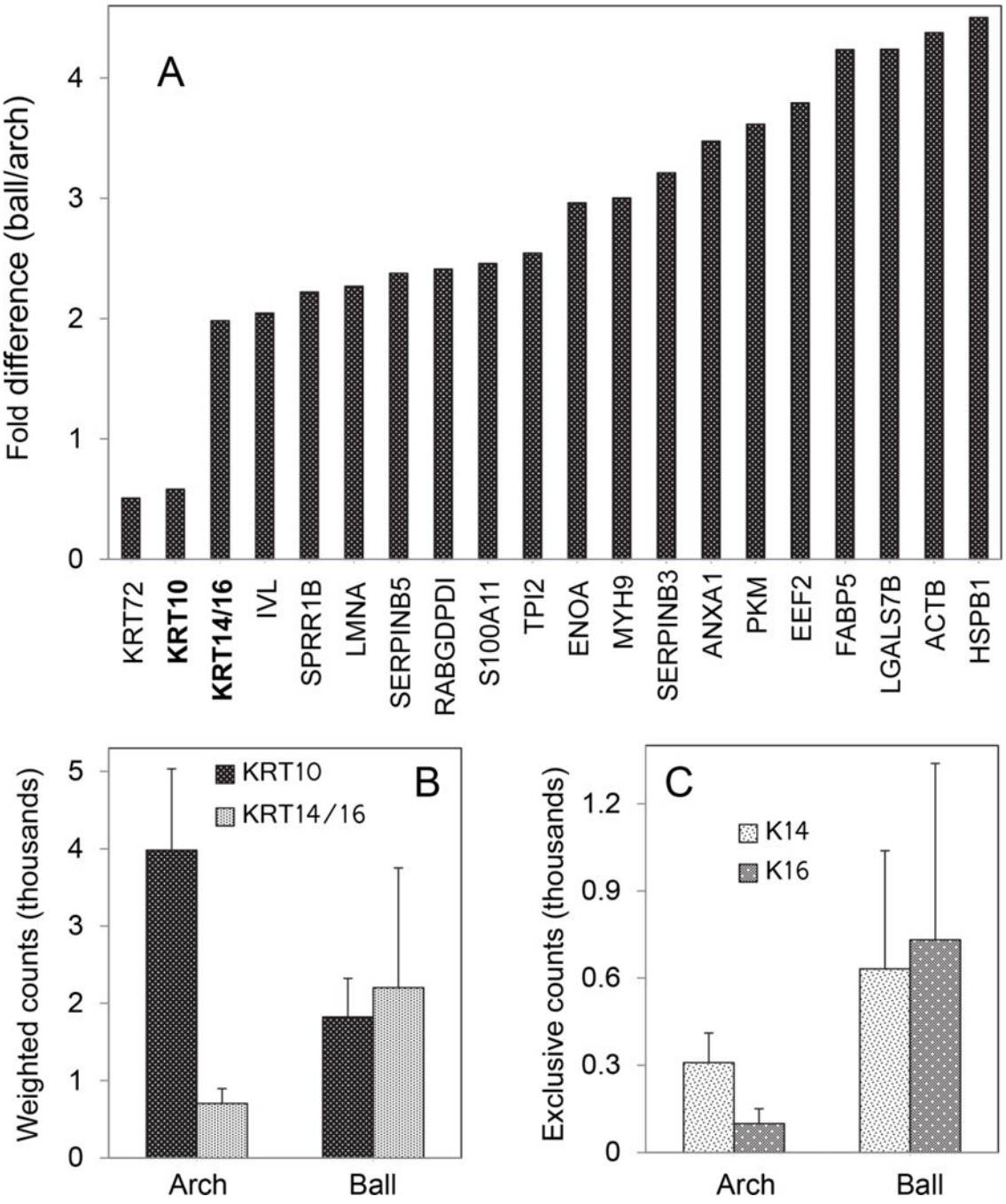

Fig. 1.

Comparison of profiles of the arch and ball of the foot in 6 normal subjects. (A) Ratios of weighted spectral counts (fold difference) from ball to arch samples among the 20 proteins judged significantly different in aggregate analysis. (B) Weighted spectral counts of K10 and K14/16 (bold in the X-axis of panel A) in the arch and ball of the foot. (C) Exclusive counts of K14 and K16 in the arch and ball of the foot.

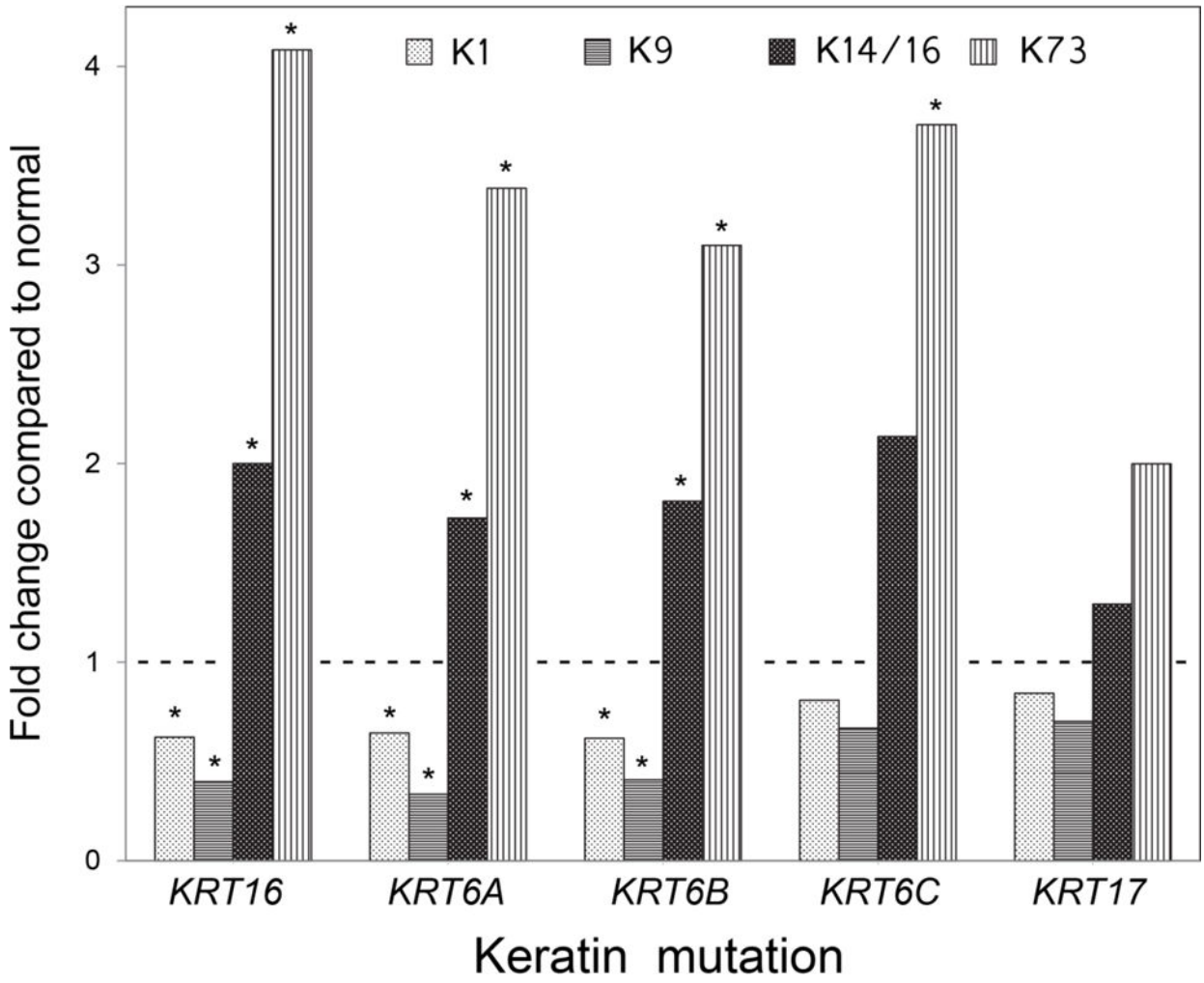

Fig. 2.

Relative keratin expression levels as a function of keratin mutation. The fold change observed in samples from each of the 5 PC groups (keratin mutations in the horizontal axis) to those in control samples are shown for K1, K9, K14/16 and K73. Asterisks indicate the ratios significantly different from control (dashed line at the value of 1).

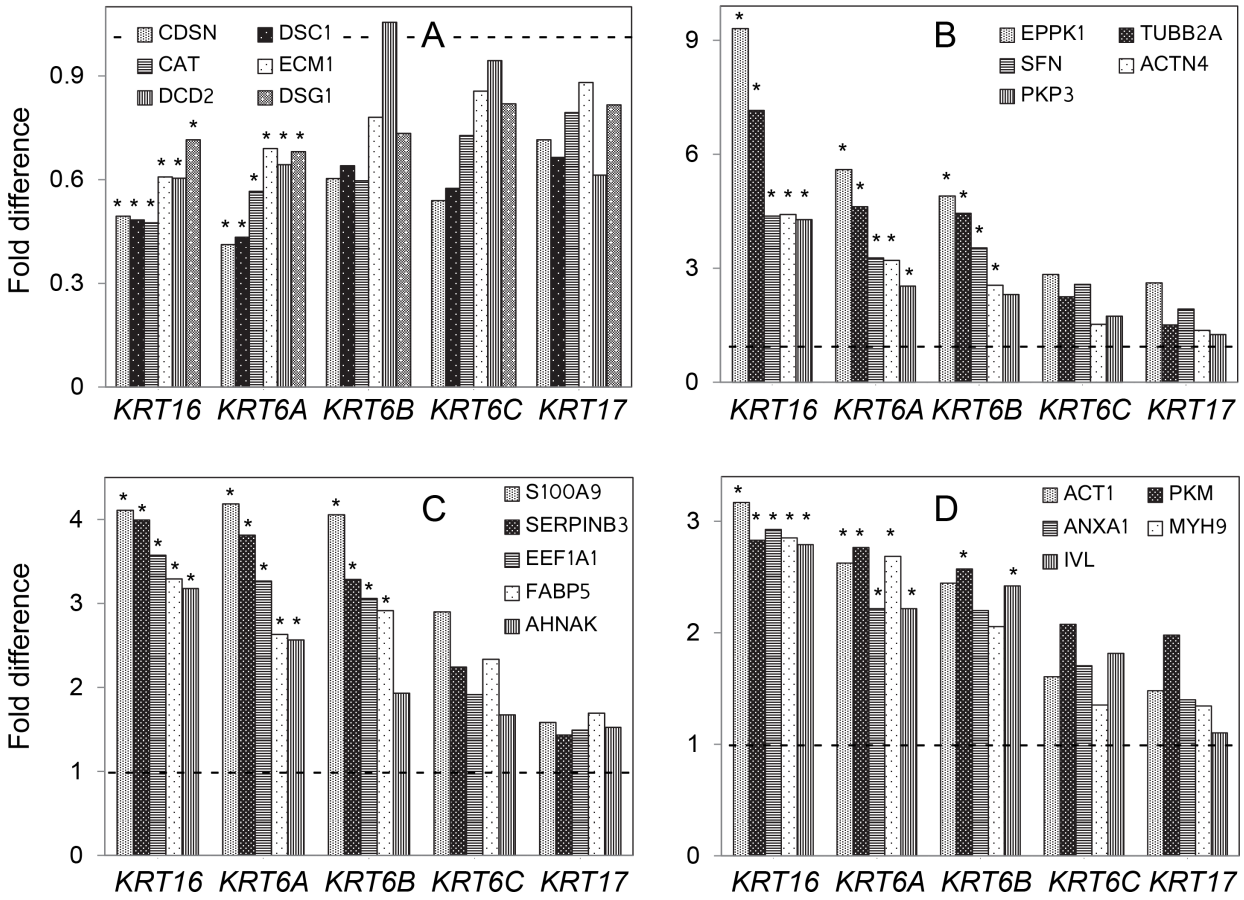

Fig. 3.

Relative expression levels of various proteins as a function keratin mutation. Keratin mutations are listed on the horizontal axis. Fold difference in the vertical axis gives the ratio of weighted spectral counts in samples with the indicated mutations compared to control. (A) Proteins with lower levels in PC samples. (B–D) Proteins with higher levels in PC samples. Asterisks indicate the ratios significantly different from control (value of 1).

Table 1

Number of proteins exhibiting differences in weighted spectral counts in two way comparisons of control (Con) and PC samples.

A. Ball	***KRT16***	***KRT6A***	***KRT6B***	***KRT6C***	***K17***
Con	99	109	36	2	4
KRT16		0	6	18	61
KRT6A			7	14	15
KRT6B				0	0
KRT6C					0
B. Arch	*KRT16*	*KRT6A*	*KRT6B*	*KRT6C*	*KRT17*
Con	5	0	0	0	0
KRT16		0	2	0	0
KRT6A			0	0	0
KRT6B				0	0
KRT6C					0

Table 2

Number of proteins with shared differences from normal samples (ball).

	KRT6A	***KRT6B***	***KRT6C***	***KRT17***
KRT16	90	35	2	2
KRT6A		36	2	4
KRT6B			2	2
KRT6C				0